IDENTIFICATION OF SCORODITE IN FINE-GRAINED, HIGH-SULFIDE, ARSENOPYRITE MINE-WASTE USING MICRO X-RAY DIFFRACTION (μXRD)

Roberta L. FLEMMING[§]

Department of Earth Sciences, University of Western Ontario, London, Ontario N6A 5B7, Canada

Kristin A. SALZSAULER*, Barbara L. SHERRIFF AND Nikolay V. SIDENKO

Department of Geological Sciences, University of Manitoba, Winnipeg, Manitoba R3T 2N2, Canada

ABSTRACT

Secondary phases precipitated during oxidation of sulfides in mine wastes can be very fine-grained and poorly crystalline, making accurate identification difficult. As part of a study to examine arsenic mobility within the arsenopyrite residue stockpile, Snow Lake, Manitoba, arsenic-rich secondary phases were examined by a combination of micro X-ray diffraction (μXRD) and electron-probe micro-analysis (EPMA). With EPMA, we found one of the secondary As-containing phases to have an Fe:As ratio of 1:1. Examination of μXRD data allowed positive identification of this phase as scorodite ($FeAsO_4 \cdot 2H_2O$). Two texturally distinct occurrences of scorodite were identified in specific areas of the polished thin sections. Type-1 scorodite occurs around grains of primary arsenopyrite, and Type-2 scorodite is disseminated throughout an amorphous iron sulfo-arsenate (AISA) matrix in highly altered material. Our observations suggest that μXRD can be used to routinely identify phases comprising <1% of the bulk sample, provided that these phases are positioned under the X-ray beam. All of the scorodite examined is very fine-grained polycrystalline material, displaying homogeneous Debye powder rings in the two-dimensional (2D) General Area Diffraction Detector System (GADDS) image, using either a 500 or 50 μm X-ray beam diameter. The homogeneous texture of fine-grained secondary scorodite makes it easily discernable from relatively coarse-grained primary minerals, which give large discrete diffraction-spots or discontinuous "grainy" Debye rings in the GADDS image.

Keywords: scorodite, arsenic, mine waste, micro X-ray diffraction, Snow Lake, Manitoba.

SOMMAIRE

Les phases secondaires précipitées au cours de l'oxydation de sulfures dans les déchets miniers peuvent bien être à granulométrie très fine et de faible cristallinité, ce qui rend une identification fiable difficile. Nous avons entrepris une étude de la mobilité de l'arsenic dans l'accumulation des réserves d'arsénopyrite à Snow Lake, au Manitoba. Dans ce contexte, les phases secondaires arsenifères sont examinées avec une combinaison de microdiffraction X (μXRD) et de micro-analyse par sonde électronique (EPMA). Avec les résultats d'analyses EPMA, nous avons identifié une des phases secondaires arsenifères contenant Fe et As dans un rapport de 1:1. Les données prélevées en microdiffraction ont permis l'identification définitive de la scorodite ($FeAsO_4 \cdot 2H_2O$). Nous notons la présence de deux manifestations texturales distinctes de la scorodite dans les lames minces polies. La scorodite de type 1 se présente comme liseré autour des grains d'arsénopyrite primaire, et la scorodite de type 2 est disséminée dans une matrice de sulfo-arsenate amorphe de fer dans le matériau le plus fortement altéré. D'après nos observations, nous pouvons utiliser la microdiffraction pour l'identification routinière des phases présentes, même en proportions moins de 1%, pourvu que des phases sont positionnées dans le faisceau. Dans tous les cas, la scorodite est polycristalline et possède une granulométrie très fine, et les anneaux de Debye homogènes dans une image produite avec un système de détecteur bi-dimensionnel GADDS, en utilisant un faisceau de rayons X de 500 ou 50 μm de diamètre. La texture homogène de la scorodite secondaire la rend facilement discernable par rapport au minéraux primaires, à grains plus grossiers, donnant des taches de diffraction ou des anneaux de Debye discontinus dans l'image produite par le détecteur GADDS.

(Traduit par la Rédaction)

Mots-clés: scorodite, arsenic, déchets miniers, microdiffraction X, Snow Lake, Manitoba.

§ *E-mail address*: rflemmin@uwo.ca
* *Present address*: Golder Associates, Redmond, Washington 98052, U.S.A.

INTRODUCTION

The identification of secondary phases precipitated during the oxidation of sulfide mine-wastes is generally difficult because of the morphology, fine-grained nature and relatively low concentration of secondary phases. Friable and very fine-grained phases are difficult to identify using conventional techniques, such as powder X-ray diffraction, which requires a relatively large amount of fine-grained material to be separated and collected. Physical separation of friable, fine-grained particles may destroy or contaminate the sample, leading to inaccurate analysis. Semicrystalline or poorly crystalline minerals precipitated during sulfide oxidation in mine wastes can be misidentified because of poor X-ray-diffraction patterns, or patterns masked by primary sulfide and silicate minerals (Jambor 2003, Gieré *et al*. 2003). The stability of ferric arsenate hinges on crystallinity, as amorphous ferric arsenate has higher solubility than crystalline scorodite ($FeAsO_4 \bullet 2H_2O$) (Krause & Ettel 1988). Scorodite, a low-solubility product of weathering of arsenopyrite, precipitates under oxidizing, acidic conditions (Dove & Rimstidt 1985, Zhu & Merkel 2001). Scorodite also is more stable than kaňkite ($FeAsO_4 \bullet 3\frac{1}{2}H_2O$), as it forms upon dehydration of kaňkite, as observed by DTA studies and field observations at Kaňk, Czechoslovakia (Čech *et al*. 1976). The low solubility of scorodite limits the concentration of arsenic in acid mine-drainage at many mine sites (Dove & Rimstidt 1985, Krause & Ettel 1988), making scorodite a desired secondary-alteration phase (Pichler *et al*. 2001). It is imperative to properly identify ferric arsenate phases to understand the solubility of arsenic minerals in the system.

Micro X-ray diffraction (μXRD) provides an effective supplementary tool for the identification of secondary minerals. In this study, μXRD was used in conjunction with electron-probe micro-analysis (EPMA) for the identification of very fine-grained products of alteration of arsenopyrite in a pile of sulfide-rich refractory mine-wastes at Snow Lake, Manitoba.

BACKGROUND INFORMATION

The Arsenopyrite Stockpile is the result of inefficient processing of refractory ore by the Nor-Acme mine between 1949 and 1958. Over 250,000 tonnes of cyanide-treated residual concentrate containing up to 60% sulfides were stockpiled for possible reprocessing. From 1959 to 2000, this residue was stored in an open waste-rock impoundment, where oxidation of sulfides and redistribution of arsenic occurred (Salzsauler 2004). In 2000, the pile was capped by layers of waste rock, clay and silt to prevent water infiltration and sulfide oxidation, resulting in the release of arsenic. Research was initiated to discover the geochemical and mineralogical processes occurring in the pile, which might cause leaching of arsenic (As) into the environment. Identification of the primary minerals and the products of their alteration is essential to the understanding of arsenic solubility in the system (Paktunc & Dutrizac 2003, Paktunc *et al*. 2004).

Crystal-structure information, for mineral identification of very fine-grained material, can be obtained by powder and single-crystal X-ray diffraction (XRD), transmission electron microscopy (TEM) and synchrotron-based techniques. Conventional powder XRD requires sizable amounts of sample and is ineffective at identifying small quantities of secondary minerals (<5%) (*e.g*., Foster *et al*. 1998). Single-crystal XRD requires individual crystals of about 0.3 mm in diameter, which are rarely attained during oxidation of mine waste. High-resolution transmission electron microscopy (HRTEM) yields crystal-structure information from selected-area electron-diffraction (SAED) patterns of very fine-grained (nm-sized) material, but it is technically demanding and can be performed only on very small samples (Hovmoller *et al*. 2002). Synchrotron methods that yield molecular-scale and crystal-scale structural information include extended X-ray-absorption fine structure (EXAFS) spectroscopy and synchrotron X-ray diffraction (SXRD). EXAFS yields the coordination environment and bond distances, but cannot supply long-range structural information (*e.g*., Strawn *et al*. 2002). Furthermore, EXAFS can generally discern only species containing >10% of the total As in the sample (Foster *et al*. 1998). SXRD is a newly emergent technique allowing *in situ* examination of nm-sized materials (Brown & Sturchio 2002, Manceau *et al*. 2002a) and mineralogical mapping (Manceau *et al*. 2002a). Synchrotron powder diffraction can ideally provide crystal-structure information by the Rietveld refinement method, but generally the sample must be polycrystalline and monomineralic (*e.g*., Scordari *et al*. 2004).

This decade has marked the emergence of laboratory-based micro X-ray diffraction (μXRD), which uses a conventional, closed-tube X-ray generator, but achieves μXRD capability through modifications to the diffraction column, sample holder, and detector. These modifications make this technique readily available to geologists for routine characterization of fine-grained materials. The Bruker D8 DISCOVER μX-ray diffractometer is a newly available instrument that can be used for examination of fine-grained materials such as the alteration-induced secondary minerals. The μXRD approach allows individual minerals to be examined *in situ*, in a rock, cut rock slab or polished section and correlated, grain for grain, with other micro-analytical data, such as from EPMA. This is made possible by the combination of four components in the μXRD instrument: theta–theta instrument geometry, Gobel mirror parallel-beam optics with exchangeable pinhole collimator (50-500 μm beam diameter), XYZ sample stage

with optical microscope – video camera, and a two-dimensional (2D) General Area Diffraction Detector System (GADDS) 15.2 cm in diameter.

Theta–theta (θ–θ) geometry allows the sample to remain stationary (flat) while the source and detector move by θ_1 and θ_2, respectively, facilitating the examination of virtually any format of sample, including loose grains. An additional advantage of the θ–θ geometry of the instrument is the ability to perform an omega scan. This operation involves simultaneously rotating the Cu source and area detector around the center of diffraction, at a fixed angle (ω) with respect to each other. Thus, from the frame of reference of the detector, the sample appears to be rotating in the opposite direction. As with conventional rotation of the sample, this has the effect of increasing the number of reflections that satisfy the Bragg diffraction condition. This operation extends the use of the Bruker D8 to a complete range of crystalline samples, from polycrystalline samples to single crystals.

Two-dimensional X-ray detection has been accomplished for many years by film techniques. Digital 2D detectors have been developed relatively recently, starting with Charge Coupled Device (CCD) area detectors in the 1990s (*e.g.*, Burns 1998), and GADDS area detectors in this decade (*e.g.,* He 2003, Tissot 2003). Area detectors are becoming a common component of modern X-ray diffractometers. The most obvious advantage of these detectors is the reduction in data-collection time over that of conventional point-counters, for the measurement of peak position and intensities, for phase identification (Tissot 2003). By simultaneously sampling two dimensions in diffraction space, area detectors can collect data that would have been missed by a point counter moving in a single line. This technique allows for more observations in the same time compared to a point counter, or alternatively, a reduction in collection time over the same diffraction space, compared to a four-circle single-crystal diffractometer. In addition, area detectors provide a measure of the texture and crystallinity of the sample, by examination of the homogeneity of the Debye rings (Helming *et al.* 2003). A sample having crystallites present in all orientations will exhibit a complete cone of diffraction, which appears as a homogeneous "powder ring" on the detector screen. A single crystal, on the other hand, will exhibit discrete diffraction-spots, one for each set of lattice planes in diffraction condition.

In this study, mine tailings from Snow Lake are examined by μXRD and EPMA. Crystal-structure information from μXRD is used in combination with chemical information from EPMA to elucidate phases in fine-grained mixtures of primary and secondary minerals. In this study, we demonstrate the flexibility and convenience of the μXRD technique over conventional XRD, and the advantage of combining crystal-structure analysis (μXRD) with chemical analysis (EPMA) at the microscopic scale.

METHODS

Sample preparation

Two types of solid material from the Arsenopyrite Residue Stockpile were available for mineralogical analysis. Refractory sulfide material was collected from the top of the Stockpile in 1998, prior to the imposition of the rock-clay cap. It was stored at room temperature in a sealed bucket until 2001, when samples were provided for this study (bucket samples). This highly altered material was considered to be the most oxidized of the residue, as the surface had been open to the atmosphere for 40 years. In March 2002, four holes were drilled into the Arsenic Residue Pile using a sonic drill; 1.5 m lengths of HQ3 core (6.25 cm diameter) encased in clear PVC sleeves were obtained and frozen until being prepared for analysis. These samples showed the oxidation state inside the residue pile after being capped for four years. The drill core was visually subdivided into oxidized, transition and reduced zones. A detailed description of sample recovery, storage and preparation is provided in Salzsauler *et al.* (2004). The sample discussed in this paper came from the transition zone and showed earlier stages of oxidation than the highly altered bucket sample.

Samples were dried at room temperature for several days. A portion of each sample was impregnated with epoxy and made into polished thin sections in the absence of water to prevent dissolution of soluble secondary phases (Salzsauler *et al.* 2004). Polished thin sections were analyzed by scanning electron microscopy (SEM), electron-probe micro-analysis (EPMA) and μXRD.

Second portions of the same samples were divided into morphological components based on appearance (color, texture and morphological association with secondary phases) under a binocular microscope. Components were handpicked from each bulk sample that contained a high ratio of secondary to primary or gangue minerals. These were finely ground and mounted onto glass slides in an acetone slurry method for conventional powder X-ray-diffraction analysis.

Scanning electron microscopy (SEM)

Grain mounts and polished thin sections were analyzed qualitatively using a Cambridge Instrument Stereoscan 120 SEM at the University of Manitoba. Energy-dispersion X-ray (EDX) spectroscopy was used to identify the major elements in each phase, and to identify possible primary and secondary phases.

Electron-probe micro-analysis

Polished thin sections were analyzed quantitatively by electron-probe micro-analysis (EPMA) using a CAMECA SX100 electron probe at the University of

Manitoba. The electron microprobe was operated at an acceleration potential of 15 kV, a beam current of 15 nA measured on a Faraday cup, with a 20 μm beam diameter, and the standards diopside (Si, Ca), arsenopyrite (Fe, As, S), chalcopyrite (Cu), gahnite (Zn), albite (Na), feldspar (K), and andalusite (Al). The raw data were corrected by the PAP correction procedure (Pouchou & Pichoir 1985). Detection limits for different components varied from 0.01 to 0.05 wt.%, and analytical precision was approximately 2% for most major elements, and 10% for minor elements.

Powder X-ray diffraction (*XRD*)

A Philips PW 1729 X-ray diffractometer operated with Ni-filtered Cu$K\alpha$ radiation generated at 40 kV and 40 mA, and 0.5° beam slit, was used at the University of Manitoba for mineral identification in the bulk samples. Diffraction patterns for selected samples were recorded by continuous scans from 6 to 90° 2θ, over 28 minutes. The major crystalline phases were identified using the JADE 6 search–match program and the International Centre for Diffraction Data (ICDD) database.

Micro X-ray diffraction

We used μXRD to identify secondary phases *in situ* in polished thin sections of the "bucket samples" and selected drill cores. The XRD data were collected using a Bruker D8 Discover diffractometer, at the University of Western Ontario. The diffractometer was operated with Cu$K\alpha$ radiation generated at 40 kV and 40 mA. A Gobel mirror parallel-optics system was used to remove $K\beta$ radiation and minimize the effect of sample displacement. A selection of beam-collimator snouts was used to reduce the $K\alpha$ beam diameter to either 500 or 50 μm. Polished thin sections were mounted on an XYZ stage, which was moved *via* remote control to analyze points previously determined by optical microscopy and SEM. An optical microscope – video camera and laser system allowed us to precisely position the sample. The θ–θ geometry of the diffractometer allowed the sample to remain stationary (flat) while the source and the detector moved independently. The angle between the sample and the source is θ_1, whereas the angle between the sample and the detector is θ_2, where $\theta_1 + \theta_2 = 2\theta$.

The sample was analyzed in Omega scan mode, where the X-ray optics (source = θ_1; detector = θ_2) were rotated through an omega angle of 21.5°. At the start of the omega scan, the source and detector where positioned at 7° and 21.5° θ, respectively. Both the source and detector were rotated clockwise, by an omega angle of 21.5°, stopping at 28.5° and 0° θ, respectively. At all points during rotation, 2θ remained constant at 28.5°. Omega scans were performed for time intervals of 8 minutes (at 500 μm beam diameter), 2 hours, and 16 hours (50 μm beam diameter).

Diffracted X-rays were detected using a GADDS 2D detector positioned at a distance of ~15 cm from the sample and intersecting a 35° segment of diffraction space, centered at 28.5° 2θ. Powder lines and diffraction spots resulting from each lattice plane {*hkl*} produced an arc of radius 2θ$_{hkl}$. The GADDS software integrated the intensity along each arc, and corrected for the effect of flat screen detection (unwarping), to create a one-dimensional plot of intensity *versus* 2θ, similar to a conventional powder-diffraction pattern. The resulting pattern was imported into the evaluation software, EVA, where phases were identified, after baseline subtraction, using the ICDD database.

RESULTS

The primary sulfide minerals of the Arsenopyrite Stockpile residue are very fine-grained (30–50 μm) arsenopyrite, pyrrhotite, pyrite and chalcopyrite (in order of decreasing abundance). Primary silicate minerals include quartz and feldspar, with minor biotite and actinolite. Figure 1 shows a typical GADDS 2D image and the resulting μXRD pattern of the dominant primary minerals, including arsenopyrite, quartz and plagioclase.

The oxidized refractory sulfide material consists of several morphologically distinct components, which allowed for *in situ* analysis by μXRD. The apparent earliest product of alteration consists of weakly to moderately altered, friable, dark greenish grey refractory sulfide material. With increasing oxidation, the refractory sulfide material is altered to friable aggregates of yellow-brown secondary sulfo-arsenate phases containing very fine-grained inclusions of resistant primary silicate minerals and highly altered primary sulfides. These sulfo-arsenates most commonly occur as aggregates of spherules measuring 300 to 500 μm in diameter, coated by a thin rim of reddish brown, gel-like amorphous iron sulfo-arsenate (AISA). In the highly altered "bucket" material, iron arsenate phases (such as scorodite) occur as inclusions in patches of lighter yellow-green amorphous iron sulfo-arsenate. As a result of a visual inspection of oxidized material in polished thin section, we found less than 5% remnant sulfides, which occurred as highly altered inclusions in amorphous AISA (Salzsauler *et al.* 2004).

The SEM data showed the dominant secondary phases in the oxidation zone containing arsenic to be iron arsenate and iron sulfo-arsenates. The composition of these phases was determined using EPMA (Table 1). The ratio of iron and arsenic in the iron arsenate is close to 1:1, suggesting that the material could be scorodite (FeAsO$_4$•2H$_2$O) (Dove & Rimstidt 1985) or kaňkite (FeAsO$_4$•3.5H$_2$O) (Robins 1987) (Table 1). As the crystallinity and hydration state of the iron arsenate could not be determined by quantitative techniques available at the time, this phase could also be an amorphous iron arsenate (Robins 1987). Significant sulfur
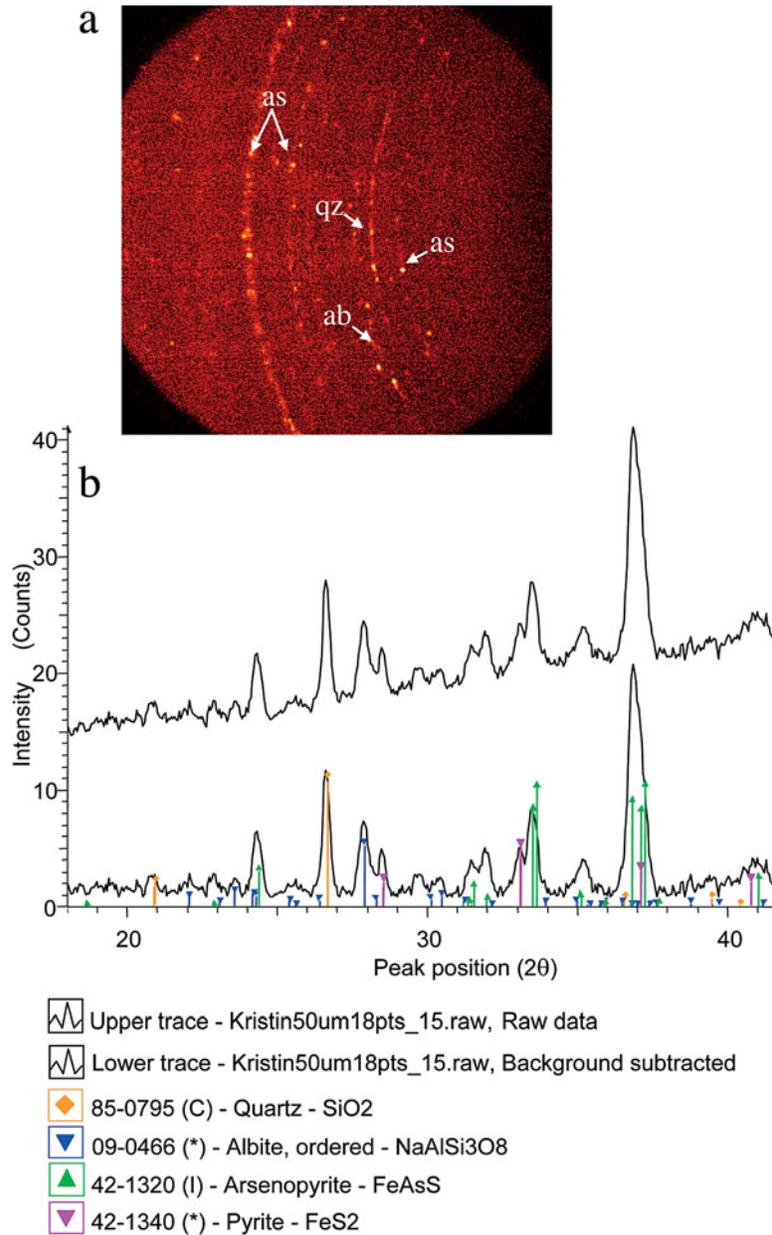
FIG. 1.   Micro X-ray-diffraction pattern (μXRD) of a polished thin section of highly altered material from the Arsenopyrite Stockpile, featuring primary minerals quartz (qz), albite (ab), and arsenopyrite (as): a) GADDS image showing powder cones and diffraction spots (phases are labeled on image). b) Corresponding plot of intensity (I) *versus* 2θ, shown with and without background correction, with ICDD data for matching phases indicated by stick patterns. Collection time: 120 min., beam diameter: 50 μm.

has been detected in hydrated ferric arsenates such as scorodite (<1.23 wt.% SO_3, Paktunc *et al.* 2004) and parascorodite (<1.53 wt.% SO_3, Ondruš *et al.* 1999). The substitution of $(SO_4)^{2-}$ for $(AsO_4)^{3-}$ results in a charge imbalance, which can be compensated by a deficiency of Fe (Paktunc & Dutrizac 2003).

Two different morphologies of iron arsenate were found using SEM and EPMA data. Type 1 consists of very fine-grained, light grayish green, spherical aggregates measuring up to 200 µm in diameter (Fig. 2) in samples of the oxidation zone taken from the drill core (Salzsauler *et al.* 2004). These aggregates form cement around primary silicate, pyrite and arsenopyrite inclusions, which measure up to 20 µm in diameter. Type 2 was found only in the highly altered "bucket" material. It forms anhedral, equant, 5 µm inclusions in later AISA phases (Fig. 3). EPMA analyses show that Type-2 material contains twice as much sulfur as Type-1 aggregates (Salzsauler 2004). It was impossible to separate Type-2 iron arsenate inclusions for analysis because of their very fine grain-size. Therefore, analysis of this material by conventional powder XRD was problematic, making it a good candidate for µXRD.

The Type-1 iron arsenate aggregates were identified as scorodite by µXRD (Fig. 4). The diffraction patterns were complicated by multiple phases as there were profuse inclusions of arsenopyrite, as well as pyrite, quartz and feldspar. The very fine-grained Type-2 iron arsenate inclusions were also confirmed to be scorodite by µXRD at both 500 and 50 µm beam diameters (Fig. 5). Diffraction patterns for Type-2 scorodite were cleaner, containing only quartz and feldspar as additional phases.

Conventional powder XRD data for a bulk sample of the highly altered material had been previously interpreted as kaňkite ($FeAsO_4•3.5H_2O$). On closer exami-

nation by µXRD, however, scorodite ($FeAsO_4•2H_2O$, orthorhombic, *Pcab*, Hawthorne 1976), could be discerned from kankite (monoclinic, *P* lattice, Čech *et al.* 1976). Values of *d* observed for scorodite (Type 2) are listed in Table 2. A least-squares, unit-cell refinement of the observed *d*-values, using LSCURIPC (Appleman & Evans 1973), yielded an orthorhombic unit-cell (*Pcab*) having dimensions *a* 8.952(5), *b* 10.342(9), *c* 10.053(9) Å, *V* 930.8(8) Å^3. These values are close to those observed previously: *a* 8.951, *b* 10.327, *c* 10.042 Å, *V* 928 Å^3 (ICDD card 37-468). Type-2 scorodite was selected for unit-cell refinement because the quartz and feldspar peaks did not overlap with the main diffraction-peaks of scorodite. The data for Type-1 scorodite, on the other hand, were compromised by peak overlap
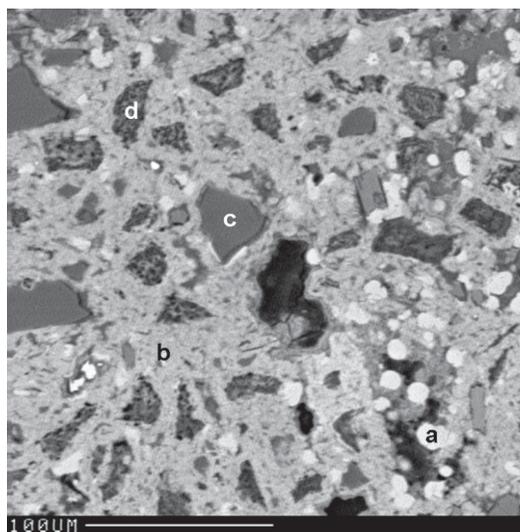
FIG. 3. Back-scattered electron image (SEM) of highly altered material from the bucket, featuring: primary Type-2 iron arsenate inclusions (a), resistant sulfide grains (c), and remnants of highly altered sulfides grains (d) in a matrix of iron sulfo-arsenate (b).

FIG. 2. Back-scattered electron image (SEM) of transition-zone material from the core, featuring: Type-1 iron arsenate (a), containing inclusions of weakly altered arsenopyrite (b).

TABLE 1. COMPOSITION OF SECONDARY PHASES, ARSENOPYRITE MINE-WASTE

Phase	Formula	Fe	As	S	N*
Ferric arsenate (1)	$Fe_{0.92}(As_{0.96}S_{0.04})O_4•2H_2O$	34.6 (±1.87)	24.7 (±1.23)	0.58 (±0.71)	45
Ferric arsenate (2)	$Fe_{0.92}(As_{0.93}S_{0.06})O_4•2H_2O$	26.0 (±0.45)	35.2 (±2.35)	1.02 (±0.40)	12
AISA		26.9 (±3.69)	26.9 (±4.57)	3.09 (±2.07)	108

* N: Number of analyses; H_2O inferred from theoretical formula of scorodite. AISA: amorphous iron sulfo-arsenate.
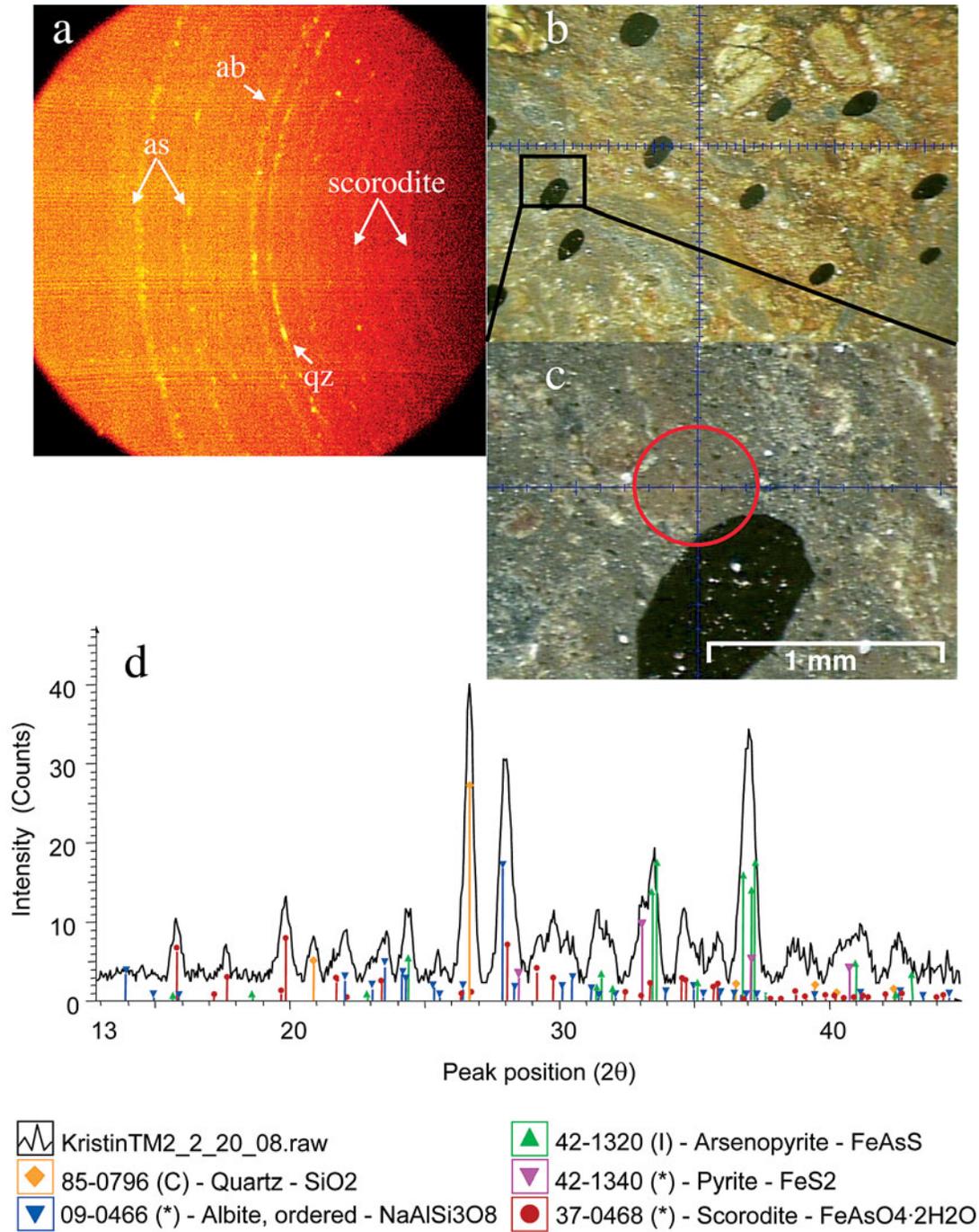
FIG. 4.   μXRD pattern of scorodite aggregates (Type 1) containing silicate and sulfide inclusions: a) GADDS image with phases indicated on image, b) minimum zoom (field of view: 13 cm), with sample located inside black box, c) maximum zoom (field of view: 2 mm), with X-ray beam diameter (500 μm) indicated by red circle, centered at crosshairs (collection time: 8 minutes), d) intensity *versus* 2θ plot, indicating matching phases.
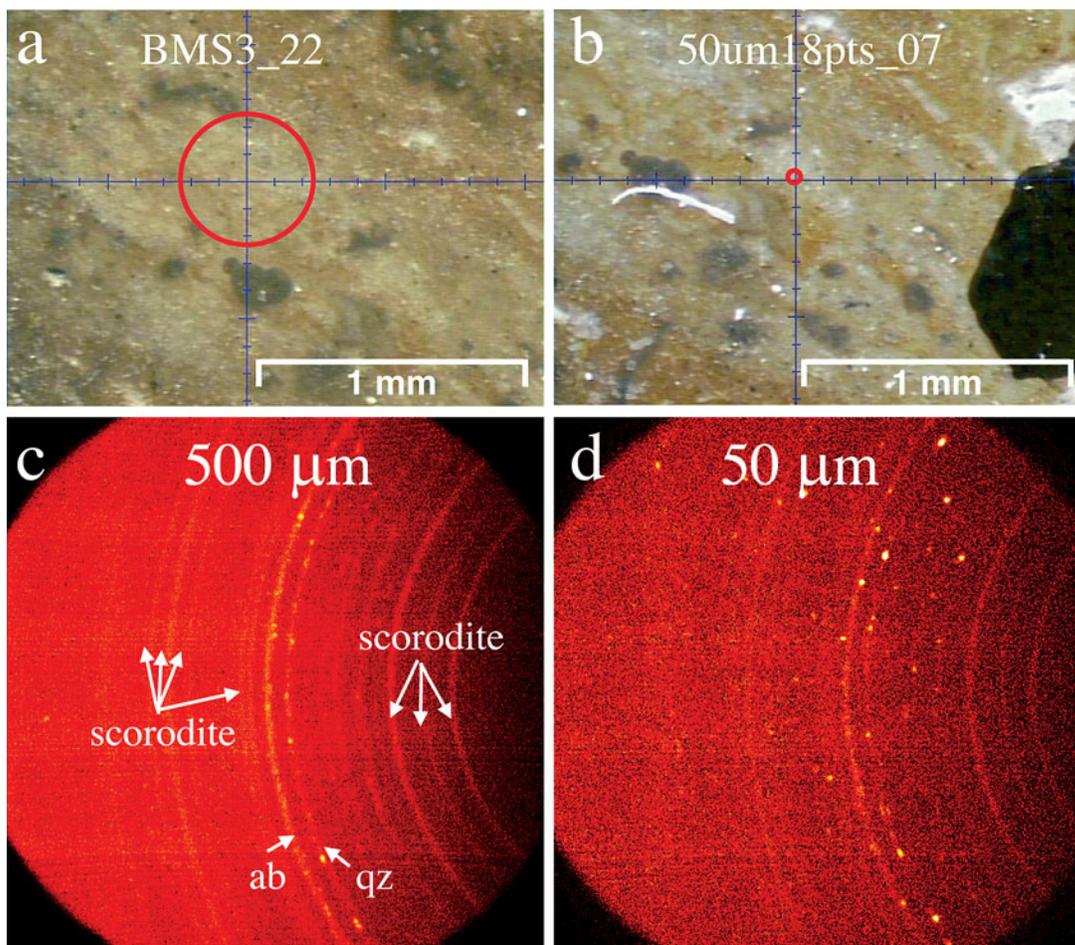
with arsenopyrite, pyrite, and additional sulfide phases, as well as quartz and feldspar. As Type-1 and Type-2 scorodite have virtually identical diffraction patterns, the Type 1*versus* Type terminology was determined to be a textural, rather than a structural distinction.

<center>DISCUSSION</center>

Comparison to conventional XRD

Although it is possible to identify scorodite and other As-containing sulfides in arsenopyrite mine-tailings and rock waste by conventional XRD of the bulk sample (Paktunc *et al*. 2004), several previous investigators were unable to do so. Pichler *et al*. (2001) did not observe scorodite in uranium-mine tailings from Rabbit Lake, Saskatchewan, but suggested it would be very difficult to identify if As-bearing phases were present in < 5% abundance in the sample. Foster *et al*. (1998) observed a "scorodite-like phase" by EXAFS it in their

mine waste, although they could not identify scorodite by conventional XRD. They attributed this difficulty to the poorly crystalline nature and low concentration of scorodite in the sample (262 ppm total As). Successful identification of minerals occurring in amounts as low as 0.25 wt % is possible by Rietveld refinement of conventional XRD data (Bish & Post 1993), but the success of this method depends on the complexity of the sample.

The μXRD aproach is more versatile than conventional XRD, requiring only a 50-500 μm area under the beam at any one time, and having the capability to examine heterogeneous samples. Using μXRD, we have been able to identify, *in situ*, phases that are otherwise difficult, if not impossible, to separate for conventional analysis. Conventional XRD can only guarantee phase identification of minerals present in >5% abundance in the bulk sample. From our observations, we consider that with μXRD, we can identify phases comprising < 1% of the bulk sample, provided that these phases
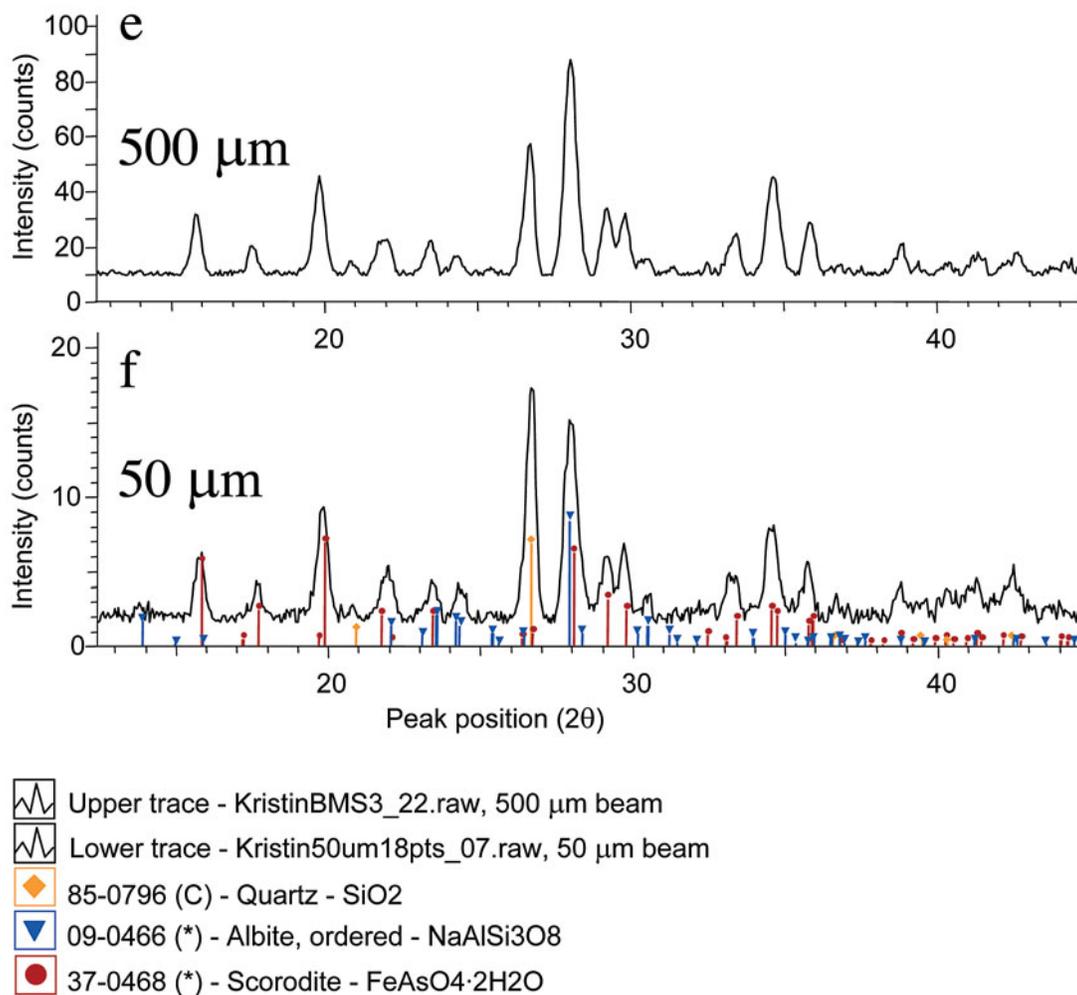
FIG. 5. μXRD pattern of highly altered refractory sulfide from "bucket material" in areas containing microcrystalline scorodite (Type 2) inclusions in AISA. Figures 5a and 5b show photomicrograph of sample locations being X-rayed. (a) Sample BMS3 (spot 22) was analyzed using a beam 500 μm in diameter, to give GADDS image d. (b) Sample BMS3 (spot 7) was analyzed at 50 μm beam diameter. In both figures, the red circle indicates the approximate beam-diameter. (c) GADDS image collected using a beam 500 μm in diameter, with a counting time of 480 s (= 8 min); (d) GADDS image collected using a beam 50 μm in diameter, with a counting time of 7192 s (= 120 min = 2 h). Note: At both scales, one can see diffraction spots of quartz and feldspar, indicating relatively few coarse-grained crystals, but one can see uniform Debye rings of scorodite, indicating a random distribution of many microcrystalline aggregates. (e) μXRD diffraction pattern of Type-2 scorodite, obtained using a 500 μm (spot 22). (f) μXRD diffraction pattern generated from spot 7, with a beam 50 mm in diameter. Intensity *versus* 2θ plots in e and f result from integration of GADDS images c and d, respectively, after background subtraction. The pattern in e, produced using a beam 500 μm in diameter, yields a maximum intensity of 90 counts in 8 min; the pattern in f, produced using a beam 50 mm in diameter, yields maximum intensity of only 18 counts in 120 min. However, peak resolution is comparable. Note: the matching phases from the ICDD database are indicated by stick patterns on the plots.

are of significant concentration under the 50–500 μm X-ray beam. In the areas selected for this study, X-ray patterns (Figs 4, 5) indicate that scorodite is present in 10–50% abundance under the X-ray beam, which is significantly higher than its abundance in the bulk sample (<5%). By μXRD, phase selection is readily accomplished by visual positioning of the sample using the optical microscope and video camera. Furthermore, phases of interest in the sample (*e.g.*, polished section) generally have been previously located during analysis by other techniques, such as the polarizing microscope or EPMA, prior to μXRD.

Comparison with synchrotron methods

Foster *et al.* (1998) observed a "scorodite-like phase" by As *K*-edge EXAFS. This identification was based on comparison of the observed EXAFS spectrum to a reference spectrum of scorodite. At this early stage in the development of EXAFS, empirical comparison to standards must be supported by evidence from other techniques such as diffraction (XRD, SXRD or SAED).

Synchrotron X-ray-diffraction (SXRD) can provide resolution about an order of magnitude higher than by μXRD, as demonstrated in recent studies of mine-waste materials (Manceau *et al.* 2002b, Walker *et al.* 2005). High-energy synchrotron radiation can produce diffraction patterns from submicrometric (nanocrystalline) material. However, this technique is technically demanding, and synchrotron beam-time must be booked months in advance. Prior to visiting a synchrotron facility, significant progress can be made in house, using μXRD in a standard X-ray lab, to identify fine-grained secondary phases.

Polycrystallinity and grain size

The μXRD approach using a GADDS detector has an additional advantage over conventional point-counters. Textural information can be gleaned from the two-dimensional GADDS image. In this study, the GADDS images (Figs. 4, 5) show high uniformity of the Debye powder rings (using both 500 and 50 μm beam diameter), revealing that both Type-1 and Type-2 scorodite form fine-grained polycrystalline phases with abundant crystallites in virtually random orientation. Scorodite powder rings are particularly pronounced in Figure 5. In contrast, primary minerals such as quartz, feldspar (Figs. 1, 4, 5) and arsenopyrite (Figs. 1, 4) show "graininess", *i.e.*, discontinuous Debye powder rings, being produced by relatively few crystallites. Bright diffraction-spots are consistent with the presence of coarse-grained crystallites. Thus, coarse-grained primary and very fine-grained secondary minerals in mine waste can be readily distinguished in a 2D GADDS image.

In Figure 5, the μXRD data are compared for Type-2 scorodite, collected at 500 and 50 μm. The secondary scorodite is so fine-grained that homogeneous Debye rings are maintained, even at 50 μm beam diameter, which has ~1000 times less sample-area than at 500 μm. This finding demonstrates the microcrystalline nature of secondary scorodite and indicates that the 5 μm particles in back-scattered-electron images are not single crystals but are polycrystalline aggregates.

Conclusions

Crystalline products of alteration in the Arsenopyrite Stockpile consist of inclusions in X-ray amorphous cements and aggregates that are friable and fine-grained. Use of μXRD enabled *in situ* identification of crystalline inclusions <5 μm in diameter, showing it to be a powerful new tool for the identification of very fine-grained, secondary phases typical of sulfide mine-wastes. Moreover, crystal-structure data supplied by μXRD can be directly compared, on a grain-to-grain basis, with micro-analytical results such as EPMA. This technique has significant potential in the study of mine wastes, as it is far more versatile than conventional XRD, technically less demanding than HRTEM, and more accessible than synchrotron methods. The μXRD approach supplies mineralogists, petrologists, chemists, and environmental scientists with a new perspective for mineralogical examination of fine-grained, microcrystalline or nanocrystalline secondary minerals that formed during alteration.

TABLE 2. VALUES OF *d* FOR SCORODITE FROM BMS3 (SPOT 22)
(BEAM 500 μm IN DIAMETER)

2θ angle peaks (°)	*d* value (Å)	Intensity (Counts)	Intensity (%)	*h k l*	Overlapping
15.7898	5.612	21.7	27.9	111	none
17.6212	5.033	10.6	13.6	002	none
19.807	4.4822	35.7	45.8	120, 200	none
21.9088*	4.0567	12.4	15.9	121, 201, 112	Ab + 3 Scd peaks
23.4392	3.7952	12.4	15.9	211	Ab
26.6678	3.3426	47.4	60.8	122	Ab
28.0194*	3.1844	78	100	212	Qtz + Ab + Scd**
29.2122	3.0570	23.9	30.6	131	none
29.7788	3.0001	22.1	28.3	113	none
32.5012	2.7547	4.5	5.8	311	none
33.3913	2.6833	14.9	19.1	123, 203	none
34.6425	2.5892	35.5	45.6	320	Scd** + Ab
35.8661	2.5037	18.8	24.1	321	none
38.8368	2.3187	11	14.2	133	Ab
40.3327*	2.2361	4.56	5.8	240?	Scd**
41.3629	2.1828	8.33	10.7	401	Scd** + Ab
42.6433	2.1201	8.1	10.4	233	Ab + Qtz
44.2684	2.0460	4.7	6	242	Scd**

* Reflections were not used in least-squares unit-cell refinement owing to peak overlap. ** Multiple peaks of scorodite (Scd).

REFERENCES

APPLEMAN, D.E. & EVANS, H.T., JR. (1973): Job 9214: Indexing and least-squares refinement of powder diffraction data. *U.S. Nat. Tech. Information Service, Doc.* **PB 216 188.**

BISH, D.L. & POST, J.E. (1993): Quantitative mineralogical analysis using the Rietveld full pattern fitting method. *Am. Mineral.* **78**, 932-940.

BROWN, G.E., JR. & STURCHIO, N.C. (2002): An overview of synchrotron radiation applications to low temperature geochemistry and environmental science. *In* Applications of Synchrotron Radiation in Low-Temperature Geochemistry and Environmental Science (P.A. Fenter, M.L. Rivers, N.C. Sturchio & S.R. Sutton, eds.). *Rev. Mineral. Geochem.* **49**, 1-119.

BURNS, P.C. (1998): CCD area detectors of X-rays applied to the analysis of mineral structures. *Can. Mineral.* **36**, 847-853.

ČECH, F., JANSA, J. & NOVÁK, F. (1976): Kaňkite, FeAsO$_4$•3H$_2$O, a new mineral. *Neues Jahrb. Mineral., Monatsh.*, 426-436.

DOVE, P.M. & RIMSTIDT, J.D. (1985): The solubility and stability of scorodite, FeAsO$_4$•2H$_2$O. *Am. Mineral.* **70,** 838-844.

FOSTER, A.L., BROWN, G.E., JR., TINGLE, T.N. & PARKS, G.A. (1998): Quantitative arsenic speciation in mine tailings using X-ray absorption spectroscopy. *Am. Mineral.* **83**, 553-568.

GIERÉ, R., SIDENKO, N.V. & LAZAREVA, E.V. (2003): The role of secondary minerals in controlling the migration of arsenic and metals from high-sulfide wastes (Berikul gold mine, Siberia). *Appl. Geochem.* **18**, 1347-1359.

HAWTHORNE, F.C. (1976): The hydrogen positions in scorodite. *Acta Crystallogr.* **B32**, 2891-2892.

HE, B.B. (2003): Introduction to two-dimensional X-ray diffraction. *Powder Diffraction* **18**, 71-85.

HELMING, K., LYUBCHENKO, M., HE, B.B. & PRECKWINKEL, U. (2003): A new method for texture measurements using a general area detector diffraction system. *Powder Diffraction* **18**, 99-102.

HOVMOLLER, S., ZOU, X.D. & WEIRICH, T.E. (2002): Crystal structure determination from EM images and electron diffraction patterns. *Advances in Imaging and Electron Physics* **123**, 257-289.

JAMBOR, J.L. (2003): Mine waste mineralogy and mineralogical perspectives of acid–base accounting. *In* Environmental Aspects of Mine Wastes (J.L. Jambor, D.W. Blowes & A.I.M. Ritchie, eds.). *Mineral. Assoc. Can., Short Course Vol.* **31,** 117-145.

KRAUSE, E. & ETTEL, V.A. (1988): Solubility and stability of scorodite, FeAsO$_4$•2H$_2$O: new data and further discussion. *Am. Mineral.* **73**, 850-854.

MANCEAU, A., MARCUS, M.A. & TAMURA, N. (2002a): Quantitative speciation of heavy metals in soils and sediments by synchrotron X-ray techniques. *In* Applications of Synchrotron Radiation in Low-Temperature Geochemistry and Environmental Science (P.A. Fenter, M.l. Rivers, N.C. Sturchio & S.R. Sutton, eds.). *Rev. Mineral. Geochem.* **49**, 341-428.

_____, TAMURA, N., MARCUS, M.A. MACDOWELL, A.A., CELESTRE, R.S., SUBLETT, R.E., SPOSITO, G. & PADMORE, H.A. (2002b): Deciphering Ni sequestration in soil ferromanganese nodules by combining X-ray fluorescence, absorption, and diffraction at micrometer scales of resolution. *Am. Mineral.* **87**, 1494-1499.

ONDRUŠ, P., SKÁLA, R., VITI, C., VESELOVSKY, F., NOVÁK, F. & JANSA, J. (1999): Parascorodite, FeAsO$_4$•2H$_2$O – a new mineral from Kaňk near Kutna Hora, Czech Republic. *Am. Mineral.* **84**, 1439-1444.

PAKTUNC, D. & DUTRIZAC, J.E. (2003): Characterization of arsenate-for-sulfate substitution in synthetic jarosite using X-ray diffraction and X-ray absorption spectroscopy. *Can. Mineral.* **41**, 905-919.

_____, FOSTER, A., HEALD, S. & LAFLAMME, G. (2004): Speciation and characterization of arsenic in gold ores and cyanidation tailings using X-ray absorption spectroscopy. *Geochim. Cosmochim. Acta* **68**, 969-983.

PICHLER, T., HENDRY, M.J. & HALL, G.E.M. (2001): The mineralogy of arsenic in uranium mine tailings at the Rabbit Lake in-pit facility, northern Saskatchewan, Canada. *Environ. Geol.* **40**, 495-506.

POUCHOU, J.L. & PICHOIR, F. (1985): "PAP" ϕ(ρz) procedure for improved quantitative microanalysis. *In* Microbeam Analysis **1985** (J.T. Armstrong, ed.). San Francisco Press, San Francisco, California (104–106).

ROBINS, R.G. (1987): Solubility and stability of scorodite FeAsO$_4$•2H$_2$O: discussion. *Am. Mineral.* **72**, 842-844.

SALZSAULER, K.A. (2004): *A Mineralogical and Geochemical Study of Arsenic in Alteration Products of Sulfide-Rich Arsenopyrite-Bearing Mine Waste, Snow Lake, Manitoba.* M.Sc thesis, Univ. of Manitoba, Winnipeg, Manitoba.

_____, SIDENKO, N.V. & SHERRIFF, B.L. (2004): Arsenic in solution and secondary phases in sulphide mine waste, Snow Lake, Manitoba. *Proc. Conf. on Water-Rock Interaction* **11**, 1381-1384.

SCORDARI, F., VENTRUTI, G. & GUALTIERI, A.F. (2004): The structure of metahohmannite, $Fe_2^{3+}[O(SO_4)_2]•4H_2O$, by in situ synchrotron powder diffraction. *Am. Mineral.* **89**, 365-370.

STRAWN, D., DONER, H., ZAVARIN, M. & MCHUGO, S. (2002): Microscale investigation into the geochemistry of arsenic, selenium, and iron in soil developed in pyritic shale materials. *Geoderma* **108**, 237-257.

TISSOT, R.G. (2003): Microdiffraction applications utilizing a two-dimensional proportional detector. *Powder Diffraction* **18**, 86-90.

WALKER, S.R., JAMIESON, H.E., LANZIROTTI, A. & ANDRADE, C.F. (2005): The speciation of arsenic in iron oxides: application of synchrotron micro-XRD and micro-XANES at the grain scale. *Can. Mineral.* **43**,

ZHU, Y. & MERKEL, B. (2001) The dissolution and solubility of scorodite, $FeAsO_4•H_2O$ – evaluation and simulation with PHREEQC. *Wiss. Mitt. Inst. Geol. TU BAF* **18**, 72-87.